

Local approach to fracture based prediction of the ΔT_{56J} and $\Delta T_{K_{Ic,100}}$ shifts due to irradiation for an A508 pressure vessel steel.

C. Bouchet¹, B. Tanguy^{1,*}, J. Besson¹ and S. Bugat²

¹Centre des Matériaux, ENSMP, UMR CNRS 7633, BP 87, Evry cedex 91003, France

²EdF les Renardières, Route de Sens - Ecuelles, Moret-sur-Loing 77250, France

* Corresponding author. Email: Benoit.Tanguy@ensmp.fr

Abstract:

A material model integrating a description of viscoplasticity, ductile damage and brittle fracture is used to simulate both the impact (Charpy) test and the toughness (CT) fracture test. The model is calibrated on the Charpy data obtained on an unirradiated A508 Cl.3 steel. It is then applied to irradiated material assuming that irradiation affects solely hardening. Comparison with Charpy energy data for different amounts of irradiation shows that irradiation probably also affects brittle fracture. The model is then used to predict the $\Delta T_{K_{Ic,100}}$ shifts for different levels of irradiation.

Introduction

The main way to determine the effect of the degradation by radiation on the mechanical behavior of the RPV steels is the use of tensile and impact (Charpy) tests, from which a reference index temperature as the DBTT or T_{56J} and its increase due to neutron irradiation can be calculated. The safety integrity evaluation based on fracture toughness lower bound is then performed assuming that the shift of RT_{NDT} due to irradiation is equal to the shift of the embrittlement indicators. This equivalence is of fundamental importance to structural integrity assessments of RPVs since such assessments are based on fracture toughness properties which are not generally measured directly. However some studies have shown large scatter in the relation between $\Delta T_{K_{Ic,100}}$ and Charpy transition temperature shifts [1]. Therefore it is important to understand this relation using micromechanical models of fracture.

Within the frame of local approach to fracture, a micromechanical analysis of the Charpy test in order to model the DBT curve was proposed, among others [2], by some of the authors [3]. Assuming that the average cleavage stress is temperature dependent beyond a given temperature, it is then possible to predict the whole Charpy energy curves [4], including the large scatter observed in the DBT range. This strategy allows one to transfer the results of the tests to larger structures and further to study the effect of different damage mechanisms as irradiation or ageing on the DBTT. The aim of this study is to predict and to compare the shifts of index temperature obtained from Charpy energy and fracture toughness curves using a micromechanical description of the damage processes.

Effect of irradiation on the transition curve and hardening properties

For a given fluence¹ and irradiation temperature, irradiation-induced embrittlement is strongly dependent of the material chemical composition, and specially on Cu, Ni, P

¹ Φ the fluence (n.cm^{-2}) of neutrons ($E > 1 \text{ MeV}$)

content [5], volume fraction of copper being an important factor in the hardening-induced embrittlement due to the defects. On the physical point of view, irradiation produces fine scale microstructures which obstruct dislocation motion [6]. The mechanisms that produce these obstacles can be separated into two groups at a macroscopic level [6, 7] : (i) hardening mechanisms, (ii) embrittlement, one of the most well-known and well-described being phosphorous segregation at grain boundaries [6]. Hardening mechanisms include matrix and age hardening. Matrix hardening is due to radiation-produced point defect clusters and dislocation loops, referred to as the matrix damage contribution [7]. Age hardening is an irradiation-enhanced formation of copper-rich precipitates. These two hardening mechanisms cause an increase of the yield strength whereas phosphorous segregation causes grain boundaries embrittlement without any increase of hardness and may be responsible for intergranular fracture [8]. It should be underlined that the micromechanical models developed in this study do not consider the embrittlement of the grain boundaries due to phosphorous segregation. Intragranular cleavage is assumed to be the prevailing mechanism.

Considering that the main irradiation effect is an increase of the hardening properties, two main cases for this effect on the material stress-strain curve were found in the literature and are schematically drawn on Fig. 1a. The first case (dashed curve labeled irr. 1) considers that the whole stress-strain curve of the unirradiated material is shifted to higher stress values by $\Delta\sigma_Y$, i.e. the strain hardening of unirradiated material does not differ from strain hardening of irradiated material [9, 10]. This case was also experimentally observed on ferritic alloys irradiated at 288°C by electron irradiation [11]. The second case considers an increase of the yield stress of $\Delta\sigma_Y$ but that the ultimate tensile stress (UTS) remains almost unaffected by irradiation (dotted curve labeled irr. 2), i.e. that the stress-strain curve in the plastic range is substantially flatter than in the unirradiated conditions. This case is reported for materials (ferritic, martensitic) irradiated by neutron irradiations at low temperatures [12] and its importance increases with decreasing irradiation temperature [13]. At high irradiation doses, it is also suggested that neutron irradiation has a similar effect as plastic strain on the strain hardening rate [14].

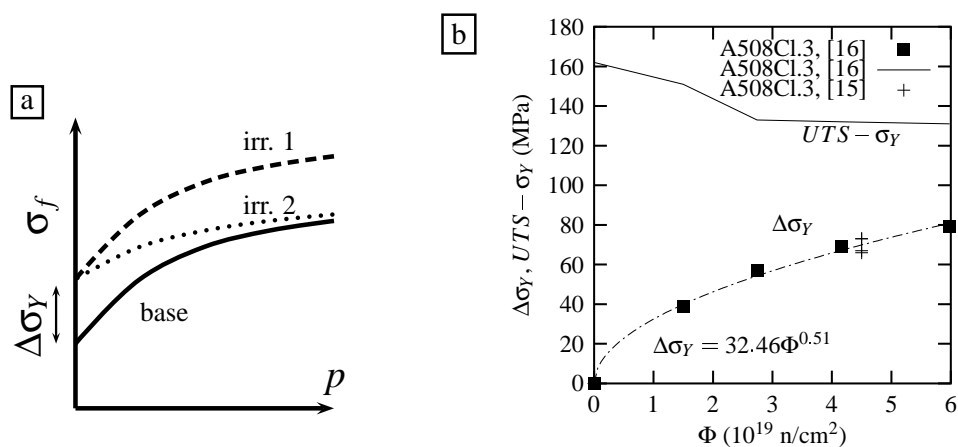


Figure 1: a) Two hypothesis concerning the evolution of the flow stress after irradiation. b) Evolution of $\Delta\sigma_Y$ and $UTS - \sigma_Y$ as a function of the irradiation flux for an A508 Cl.3 steel (base metal) ($T_{\text{test}} = 300^\circ\text{C}$) [16].

The choice of the appropriate case is undoubtedly strongly dependent of the material considered: in the interpretation of irradiation effects on low temperature fracture toughness, the second case was considered for an A533B steel [17] whereas it was the first case for an A508 Cl3 steel in [10].

The variation of the yield stress and the difference between the ultimate stress and the yield stress for an A508 Cl3 steel from the french surveillance program [15, 16] with a chemical composition close to the unirradiated material considered in this study and their evolutions with irradiation flux are reported on Fig. 1b. The variation of the yield stress with fluence is well represented by a power-law expression, $\Delta\sigma_Y = h\Phi^n$. A value of 0.51 is obtained for n which is representative of the low doses regimes [12]. Data shown on Fig. 1b show that the first case is the most satisfactory hypothesis for fluence up to 6.10^{19}n/cm^2 (i.e. $\Delta\sigma_Y \sim 80$ MPa for the steel investigated) even if the $UTS - \sigma_Y$ value slightly decreases with increasing radiation fluence. Therefore the first case will be the only one treated in the present study.

Considering both the impact and fracture toughness properties, it is well known that irradiation embrittlement induces an increase of the DBTT [1, 6, 8, 10, 17, 18]. Moreover, for impact properties a general trend is a decrease of the upper shelf energy (USE). Based on experimental evidences, linear correlations between yield stress increase under irradiation and the DBTT shift on Charpy energy curves, $\Delta T_X = \alpha_X \Delta\sigma_Y$, have been proposed in the litterature. In the French surveillance program, the shift of the index T_{56J} is considered [8] whereas T_{41J} is used in the American regulations. From the experimental values given in [5, 8, 16, 19] linear correlations between ΔT_{56J} , ΔT_{41J} and $\Delta\sigma_Y$ for various RPV base metals was established: $\Delta T_{56J} = 0.60\Delta\sigma_Y$ and $\Delta T_{41J} = 0.53\Delta\sigma_Y$ (see Fig. 2). The ΔT_{56J} correlation will be considered as the reference experimental database to which the predictions developed in this study for Charpy tests will be compared. For the fracture toughness tests, the level of $100\text{ MPa}\sqrt{\text{m}}$, which is also considered in the Master curve approach to define the reference temperature, T_0 , will be used. Based on the fracture toughness test simulations the predicted shift of the index $\Delta T_{K_{Ic},100}$ due to irradiation will be determined and compared to the shift ΔT_{56J} .

Modelling of the ductile to brittle transition

The behavior of the reference unirradiated A508 steel of this study is presented in the following. The material model consists of three parts: (i) a temperature and strain rate dependent viscoplastic model describing the behavior of the undamaged material, (ii) a model for ductile tearing, (iii) a model for brittle failure.

The viscoplastic behavior has been described in [20]. The model is identified for strain rates between 10^{-4} and 4000 s^{-1} , temperature between -196 and 300°C and plastic strains up to 1.0 using the Bridgman analysis.

The model for ductile failure is presented in [21] and is not detailed here. A modified Rousselier model, which is able to handle strain rate and temperature dependence, is used to model void nucleation and growth and final failure. The constitutive equations lead to softening up to crack initiation and propagation so that a material scale length is required. In the following, this length, h , is identified to the mesh size which must be adjusted. The model was fitted using notch tensile bars (NT) at room temperature [3]. The following model parameters were used: $q_R = 0.89$, $D_R = 2.2$ and $h = 100\text{ }\mu\text{m}$.

The description of brittle failure is derived from the Beremin model which is adapted

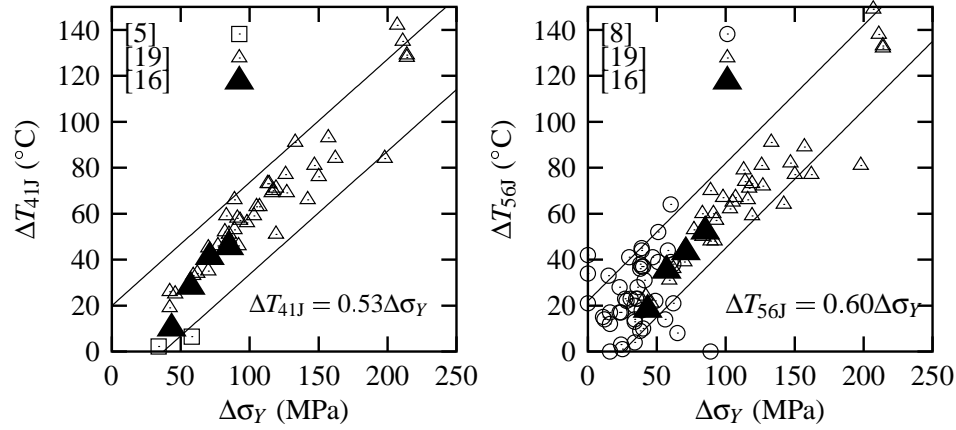


Figure 2: Evolution of temperature indexes, ΔT_{41J} and ΔT_{56J} as a function of $\Delta \sigma_Y$ for base metal.

to account for: (i) the partial unloading of the specimen when the crack propagates, (ii) the temperature dependence of the model parameters which were considered as constant in the original model. The full description is given in [4]. The parameters of the model for brittle fracture have been identified using notched tensile bars (NT) tested at low temperature ($T < -150^\circ\text{C}$): $m = 17.8$, $k = 4$ and $\sigma_u = 2925 \text{ MPa}$.

The transition is modeled by simulating ductile tearing and by post-processing the results in order to obtain the brittle failure probability. There is therefore no specific model for the transition. However it is necessary to use a phenomenological dependence with temperature for σ_u above a threshold temperature ($\approx -80^\circ\text{C}$) to model the sharp upturn of the Charpy transition curve [4] (Fig. 4). This apparent effect of temperature on the cleavage mechanism is not the scope of this paper. The simulation is based on the finite element (FE) method. Details can be found in [3].

Simulation of the ductile to brittle transition

Using the previously described models and the hypothesis that the effect of neutron irradiation on DBTT shifts can be quantitatively assessed in terms of the effects of radiation on the yield properties of the material, it becomes possible to model the effect of irradiation on the ductile to brittle transition curves and to forecast quantitatively the Charpy energy or fracture toughness versus temperature curves.

In order to simulate the whole DBT curve, FE modelling of Charpy-V notch and CT specimens have been carried out in the temperature ranges $[-140^\circ\text{C} : +100^\circ\text{C}]$ and $[-100^\circ\text{C} : +100^\circ\text{C}]$, respectively. The increase of yield stress due to irradiation in the whole temperature range investigated is then needed. A first approach is to consider that the hardening observed at one temperature is the same in the whole temperature range [10]. Hereafter the flow stress of the unirradiated material is modified by adding a contribution representing the irradiation effect which is expressed as: $\Delta \sigma_Y^{300} \times g(T)$ where $\Delta \sigma_Y^{300}$ is the increase of the yield stress at 300°C and $g(T)$ a function of the temperature

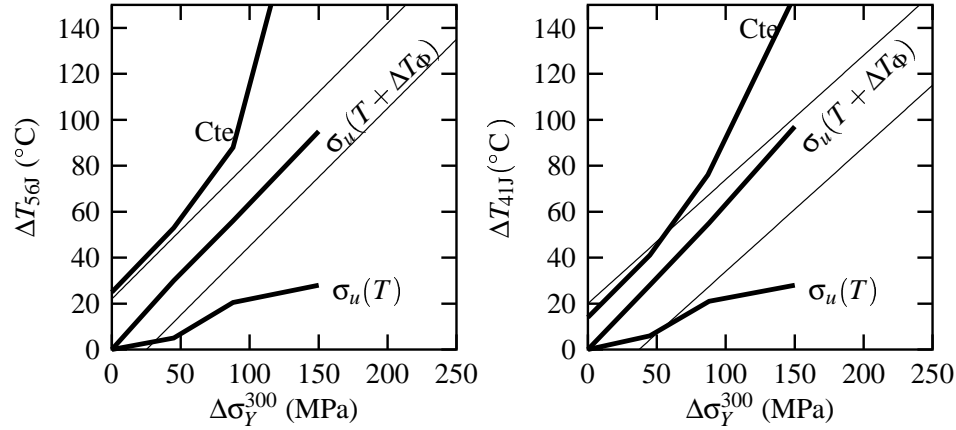


Figure 3: Prediction of ΔT_{56J} and ΔT_{41J} . Three hypothesis are used for the parameter σ_u : (i) constant value (low temperature value for the unirradiated material), (ii) temperature dependent σ_u (unirradiated material), (iii) temperature and irradiation dependent σ_u (Fig. 4). Thin lines indicate the experimental range.

identified on experimental results [16]. Full 3D computations have been made for both geometries. Calculations are then post-processed in order to simulate the ductile-brittle transition behavior.

Simulation of the Charpy ductile to brittle transition curve

In a previous study [22], the Charpy transition curve was simulated for different values of $\Delta \sigma_Y$, i.e. for different amount of irradiation flux, equal to 45 (low irradiation level), 88 (mean irradiation level) and 150 MPa (high irradiation level). For irradiation levels higher than those reported on Fig. 1b and up to $\Delta \sigma_Y = 150$ MPa, it is supposed that the saturation in irradiation hardening or the change of deformation mode [12, 23] are not active which seems to be confirmed by the data for an A533B steel reported in [12].

As a general trend, the increase of the flow stress has two consequences: (i) stresses in the material increase causing earlier brittle failure, (ii) the macroscopic load on the Charpy specimen increases causing an increase of the dissipated energy in the ductile regime so that the USE also increases. The USE is computed by propagating the ductile crack through the whole Charpy specimen.

Results for the shifts obtained on the reference temperatures, ΔT_{56J} and ΔT_{41J} are reported on Fig. 3. As the trend observed for both temperature indexes are similar, comments will focus on the ΔT_{56J} index (Fig. 3a). For the three $\Delta \sigma_Y$ values considered, it is shown that ΔT_{56J} is always underestimated assuming that σ_u is unaffected by irradiation. Assuming that σ_u is a constant equal to the low temperature value for the unirradiated material (2925 MPa) gives a conservative estimation of ΔT_{56J} .

To obtain the correct temperature shift given in Fig. 2b, σ_u has to be assumed to be also affected by irradiation. The parameter for the irradiated material is expressed as: $\sigma_u^{irr} = \sigma_u(T + \Delta T_\Phi)$.

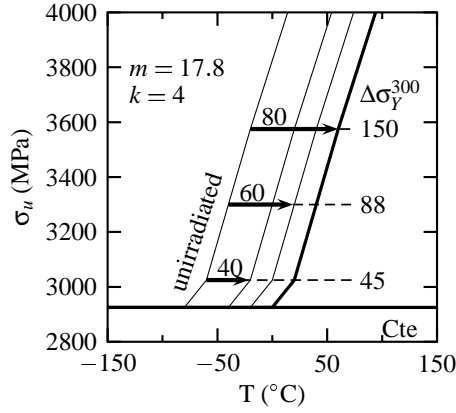


Figure 4: Variation of σ_u as a function of temperature for the unirradiated material and for irradiation level corresponding to an increase of the yield stress equal to 45, 88 and 150 MPa. Arrow indicates the temperature shift, ΔT_Φ , caused by irradiation.

The shift ΔT_Φ depends on the level of irradiation, it is calculated in order to represent the experimental correlation $\Delta T_{56J} - \Delta \sigma_Y$ (Fig. 2b) and is given in Fig. 4 for the three considered values of $\Delta \sigma_Y$. It is shown in Fig. 3b, that the prediction for ΔT_{41J} is in reasonable agreement with experimental bounds up to the maximum $\Delta \sigma_Y$ considered in this study (150 MPa).

Simulation of the fracture toughness ductile to brittle transition curve

The same methodology has been applied to simulate the fracture toughness curve: the evolution of σ_u^{irr} determined to fit the correlation $\Delta T_{56J} - \Delta \sigma_Y$ was applied to predict the shift of $T_{KIC,100}$ as a function of $\Delta \sigma_Y$. The ability of the model to predict fracture toughness for the unirradiated material using the $\sigma_u(T)$ relation obtained from Charpy data was shown in a previous study [24]. As in this study no tests have been performed on the A508 Cl3 steel after irradiation, data from literature on similar materials [10, 15] were used for comparison with the model predictions. The effect of irradiation on the shifts of the reference temperature, $T_{KIC,100}$ is reported on Fig. 5 .

For $\Delta \sigma_Y = 45$ and 88 MPa, a good agreement is obtained between the model predictions and available experimental data (see Fig. 5 a and b). The $\Delta T_{KIC,100}$ shift values obtained considering the 50% failure probability prediction are reported on each graph and a comparison with ΔT_{56J} is made in tab. 1.

The predicted $\Delta T_{KIC,100}$ values are higher than the shifts ΔT_{56J} , i.e. ΔRT_{NDT} . The

Table 1: Comparison between ΔT_{56J} and predicted $\Delta T_{KIC,100}$ shifts

$\Delta \sigma_Y$ / MPa	ΔT_{56J} / °C	$\Delta T_{KIC,100}$ / °C	$\Delta T_{KIC,100} - \Delta T_{56J}$ / °C
45	27	49	+22
88	53	73	+20
150	90	104	+14

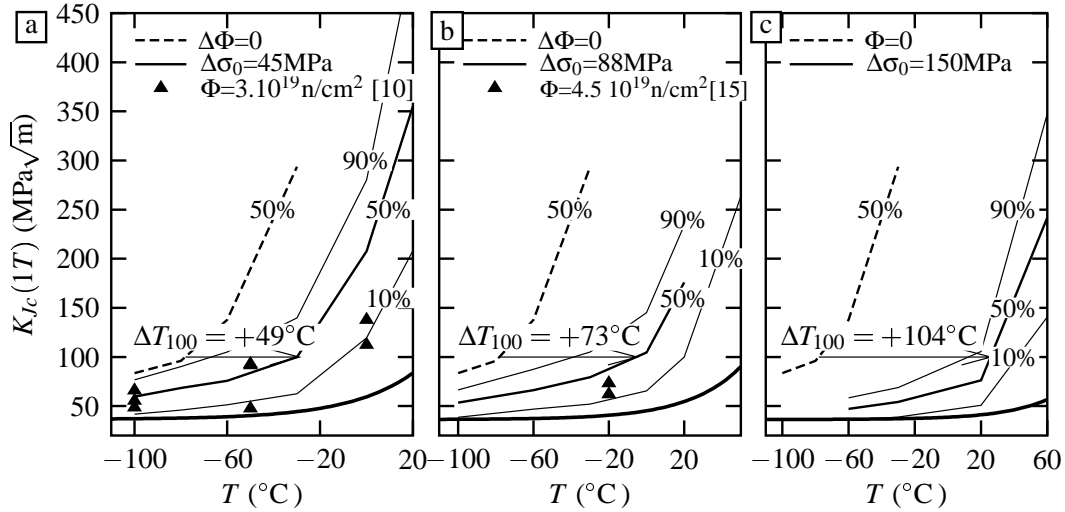


Figure 5: Comparison of the unirradiated and irradiated predicted fracture toughness curve bounds of neutron-irradiated A508 cl.3 steel as a function of temperature for different increases of the yield stress, $\Delta\sigma_Y$. a) $\Delta\sigma_Y = 45$ MPa, b) $\Delta\sigma_Y = 88$ MPa, c) $\Delta\sigma_Y = 150$ MPa. The calculated temperature shifts at $100 \text{ MPa}\sqrt{\text{m}}$ referring to the unirradiated state are reported on each graph. The ASME K_{Ic} curves are represented for irradiated material in thick line ($RT_{NDT}^{unirr} = -27^\circ\text{C}$)

difference decreases with increasing $\Delta\sigma_Y$.

The shift $\Delta T_{K_{Ic},100}$ being more important than the shift ΔT_{56J} (ΔRT_{NDT}) from the result obtained from the methodology developed in this study, the conservatism of the ASME K_{Ic} curve has to be checked for the irradiated material. The ASME K_{Ic} curve is plotted on each graph of Fig. 5) (thick line) using the ΔT_{56J} values given in tab. 1 and the initial $RT_{NDT}^{unirr} = -27^\circ\text{C}$. It is shown that in the investigated range of $\Delta\sigma_Y$, the model predictions are always less conservative than ASME curve which remains a lower bound despite that the shifts obtained from the predicted fracture toughness data are higher than those predicted from the Charpy impact data.

Conclusions and discussion

The ductile to brittle transition characterized by the Charpy test and Compact Tension fracture toughness test has been modeled in the case of a RPV steel using constitutive equations for viscoplasticity, ductile tearing and brittle failure. The transition curve of the based unirradiated material can be modeled provided the parameter σ_u of the Beremin model is considered to be an increasing function of temperature.

Irradiation hardens the material causing an increase of the stresses thus causing earlier brittle failure. This effect cannot account for the whole experimental reference temperature shift ΔT_{56J} . It is therefore necessary to consider that irradiation also affects the position of the $\sigma_u(T)$ curve on the temperature axis. Irradiation effect is then equivalent to a cooling of the material, the $\sigma_u(T)$ curve being shifted towards higher temperatures. The micromechanical mechanism needs however to be identified.

Using the value of $\sigma_u(T + \Delta T_\Phi)$ determined from Charpy data, the shifts of fracture

toughness index temperature for different level of hardening corresponding to different level of irradiation were found to be higher than the corresponding shifts obtained from Charpy energy curves. The difference decreases with increasing hardening. However the ASME K_{Ic} curve with $\Delta RT_{NDT} = \Delta T_{56J}$ remains a lower bound for the CT(1T) fracture toughness data.

References

- 1 Onizawa, K. and Suzuki, M., In: *Effects of radiation on materials: 20th Inter. Symp.*, Rosinski, S., Grossbeck, M., Allen, T. and Kumar, A. (Eds.). ASTM STP 1405, 79–96, 2001.
- 2 Parrot, A., Forget, P. and Dahl, A., In: *Proceedings of PVP 2003, Fatigue, Fracture & Damage.*, Cleveland, Ohio, USA, 2003.
- 3 Tanguy, B., Besson, J., Piques, R. and Pineau, A., In: *From Charpy to present impact testing*, François, D. and Pineau, A. (Eds.).ESIS Publication 30, 461–468, 2002.
- 4 Tanguy, B., Besson, J., Piques, R. and Pineau, A., *Engng Fract Mech, to be published*, 2004.
- 5 Haggag, F. M., In: *Effects of Radiation on Materials: 16th Inter. Symp.*, ASTM STP 1175, Kumar, A. S., Gelles, D. S., Nanstad, R. K. and Little, E. A. (Eds.). 172–185, 1993.
- 6 Nikolaev, Y. A., Nikolaeva, A. V. and Shtrombakh, Y. I., *Int. J. Pres. Ves. and Piping*, **79**, 619–636, 2002.
- 7 Wagenhofer, M., Gunawardane, H. P. and Natishan, M. E., In: *Effects of Radiation on Materials: 20th Inter. Symp.*, ASTM STP 1045, Rosinski, S. T., Grossbeck, M. L., Allen, T. R. and Kumar, A. S. (Eds.). ASTM, 97–108, 2001.
- 8 Brillaud, C. and Hedin, F., In: *Effects of radiation on materials: 15th Inter. Symp.*, Stoller, R., Kumar, A. and Gelles, D. (Eds.). ASTM STP 1125, 23–49, 1992.
- 9 Margolin, B., Gulenko, A., Nikolaev, V. and Ryadkov, L., *Int. J. Pres. Ves. and Piping*, **80**, 817–829, 2003.
- 10 Al Mundheri, M., Soulat, P. and Pineau, A., *Fatigue Fract. Engng. Mater. Struct.*, **12** (1), 19–30, 1989.
- 11 Farrell, K., Stoller, R., Jung, P. and Ullmaier, H., *J. Nuclear Materials*, **279**, 77–83, 2000.
- 12 Byun, T. and Farrell, K., *J. Nuclear Materials*, **326**, 86–96, 2004.
- 13 Odette, G., Yamamoto, T., Rathbun, H., He, M., Hribernik, M. and Rensman, J., *J. Nuclear Materials*, **323**, 313–340, 2003.
- 14 Byun, T. and Farrel, K., *Acta mater.*, **52**, 1597–1608, 2004.
- 15 Trouvain, C. Technical report, CEA, Saclay, 1989.
- 16 EDF. Edf industry-nuclear generation division corporate laboratorie, private communication, 2003.
- 17 Parks, D., *J Engng Mater Technology*, 30–36, 1976.
- 18 Brillaud, C., Grandjean, Y. and Sallet, S., In: *Effects of Radiation on Materials: 20th Inter. Symp.*, ASTM STP 1045, Rosinski, S. T., Grossbeck, M. L., Allen, T. R. and Kumar, A. S. (Eds.). ASTM, 28–40, 2001.
- 19 Sokolov, M. and Nanstad, R. Technical report, ORNL, NUREG/CR-6609, 2000.
- 20 Tanguy, B., Piques, R., Laiarinandrasana, L. and Pineau, A., In: *EUROMAT 2000, Advances in Mechanical Behaviour. Plasticity and Damage*, Miannay, D., Costa, P., François, D. and Pineau, A. (Eds.). Elsevier, 499–504, 2000.
- 21 Tanguy, B. and Besson, J., *Int J Frac*, **116**, 81–101, 2002.
- 22 Bouchet, C., Tanguy, B., Besson, J. and Bugat, S., In: *IWCMM 13*. Magdeburg, 2003.
- 23 Farrell, K. and Byun, T., *J. Nuclear Materials*, **318**, 274–282, 2003.
- 24 Tanguy, B., Besson, J., Bouchet, C. and Bugat, S., In: *PVP ASME*. San Diego, 2004.